Macromolecules

Article

pubs.acs.org/Macromolecules

Characteristics of Lamellar Mesophases in Strongly Segregated Broad Dispersity ABA Triblock Copolymers

Adam K. Schmitt and Mahesh K. Mahanthappa*

Department of Chemistry, University of Wisconsin−Madison, 1101 University Ave., Madison, Wisconsin 53706, United States

Supporting Information

ABSTRACT: We report the synthesis and characterization of a series of 13 strongly segregated poly(lactide-*b*-1,4-butadiene-*b*-lactide) (LBL) triblock copolymers, in which a broad dispersity center B segment ($Đ = M_w/M_n \sim 1.7-1.9$) is embedded between two narrow dispersity L end blocks ($Đ \leq 1.20$). Derived from chain transfer ring-opening metathesis polymerization (ROMP-CT) of 1,5,9-cyclododecatriene in the presence of 1,4-diacetoxy-2-butene, α,ω-dihydroxytelechelic poly(1,4-butadienes) serve as ring-opening transesterification polymerization (ROTEP) macroinitiators for the parallel synthesis of LBL triblock copolymers with $M_n = 12.4-28.7$ kg/mol and volume fractions $f_B = 0.44-0.79$. By determining the Flory−Huggins interaction parameter $\chi_{LB} = 0.192$ at 155 °C from mean-field theory analyses of synchrotron X-ray scattering profiles for a narrow dispersity LB diblock copolymer, we estimate that the segregation strengths associated with the broad dispersity LBL copolymers range $\chi_{LB}N = 35.1-83.6$. As compared to their narrow dispersity analogues reported herein, broad B segment dispersity shifts the composition-dependent lamellar phase window in LBL triblocks to higher values of $f_B = 0.52-0.75$. Contrary to previous reports of substantial dispersity-induced, lamellar domain spacing dilation in weakly segregated AB diblock and ABA triblock copolymers, strongly segregated LBL copolymers exhibit surprisingly similar domain sizes and scaling relations ($d \propto N^{0.72\pm0.06}$) to their narrow dispersity analogues. This finding suggests that the magnitude of χ_{AB} determines the moment of the molar mass distribution that controls the observed lamellar domain spacing.

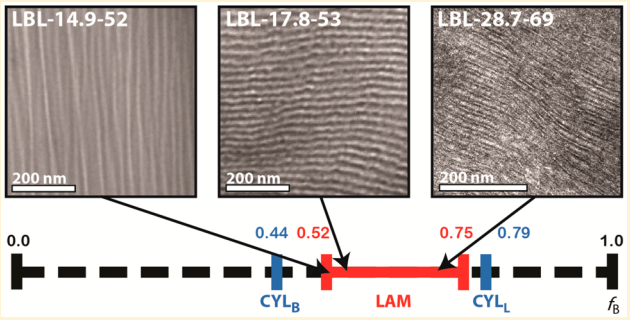

INTRODUCTION

The useful, self-assembled morphologies adopted by block copolymers have motivated many detailed theoretical and experimental studies of their microphase separation behavior at the nanoscale.[1,2] As a consequence of the chemical incompatibility of their constituent homopolymer segments, AB diblock and A/B multiblock copolymers adopt technologically useful ordered phases that include lamellae (L), hexagonally packed cylinders (C), spheres packed on a body-centered cubic lattice (S), and the triply periodic double gyroid ($Ia\bar{3}d$ or Q^{230}) and *Fddd* (O^{70}) network phases.[3] Mean-field theory treatments of perfectly monodisperse A/B block copolymer phase behavior reveal that the observed ordered morphologies and their underlying thermodynamic stabilities are parametrized by the copolymer composition or volume fraction, $f_A = 1 - f_B$, and the segregation strength $\chi_{AB}N$, wherein N is the total segment density-normalized degree of polymerization and χ_{AB} is the interaction energy associated with unfavorable A/B monomer contacts.[4] For strongly segregated, linear A/B multiblock copolymers, these theories predict that the lamellar phase is typically observed in the composition range $f_A \sim 0.35-0.65$ when the statistical segment lengths of the constituent homopolymer segments are equal ("conformational symmetry").[5,6] In the strong segregation limit ($\chi N \gtrsim 50-100$),[7−9] the lamellar microdomain spacing for AB diblocks scales as $d \propto N^{2/3}$.[10] For ABA triblock copolymers, Matsen and Schick showed that $d \propto N^{0.68}$.[11] Over the past 20 years, numerous experimental studies of narrow dispersity copolymers ($Đ = M_w/M_n < 1.1$) derived from anionic polymerizations have largely confirmed these theoretical predictions.[12−14]

Recently developed "controlled"/living,[15,16] degenerate transfer,[17,18] and change of mechanism polymerization (ChOMP)[19,20] methods enable access to a wide range of block copolymers with new chemical functionalities and unusual bulk properties. An essential feature of all of these synthetic methodologies is that they afford polymeric materials with well-defined end groups, which enable sequential addition reactions of chemically dissimilar monomers to form block copolymers. For example, these polymer syntheses afford access to new optoelectronic copolymers,[21] sustainable materials derived from biorenewable feedstocks,[22,23] and environmentally friendly, degradable block copolymers.[24,25] While these synthetic approaches permit control over the average molecular weights and compositions of the resulting materials, the molar mass distributions ($Đ = M_w/M_n$) of these copolymers can be quite broad.[2] Thus, these new synthetic strategies furnish block

Received: March 26, 2014
Revised: June 7, 2014
Published: June 25, 2014

   dx.doi.org/10.1021/ma5006233 | Macromolecules 2014, 47, 4346−4356

copolymers, wherein the constituent homopolymer segments exhibit dispersities in the range $Đ = 1.3-2.0$. In some cases, the broad segmental dispersities in these commercially produced copolymers lead to superior polymer processabilities, bulk mechanical properties, and unexpected photonic properties.[26−28]

Recent, detailed studies of AB diblock[29−35] and ABA triblock[36−39] copolymers with broad dispersity B segments and narrow dispersity A segments have highlighted differences in their phase behaviors as compared to their narrow dispersity analogues. At intermediate and weak segregation strengths ($\chi_{AB}N \leq 50$), segmental dispersity in these materials does *not* impede their self-assembly into well-defined cylindrical and lamellar morphologies. However, the composition-dependent morphological windows are shifted as compared to their narrow dispersity analogues and the microdomain spacings dilate by as much as 100%. The ABA triblock architecture accentuates many of these effects. Widin et al. also discovered that nearly symmetric composition poly(styrene-*b*-1,4-butadiene-*b*-styrene) (SBS) copolymers, comprising a broad dispersity B block ($Đ \sim 1.73-1.90$) flanked by two narrow dispersity S blocks ($Đ \leq 1.20$), form a remarkably stable disordered bicontinuous morphology.[38] Surprisingly, these samples exhibit a nearly invariant domain spacing $d \sim 39$ nm when $M_{n,total} = 12.3-36.1$ kg/mol. Contrary to expected analogies between small molecule crystallization and block copolymer microphase separation, the order−disorder transition temperatures (T_{ODT}) of these broad dispersity block copolymers are also much higher than those of their narrow dispersity analogues.[35,37,39] For example, the critical segregation strength for microphase separation in the aforementioned SBS triblocks was reported by Widin et al. to be $(\chi_{AB}N)_{ODT} \sim 4.54$, as compared to $(\chi_{AB}N)_{ODT} = 17.9$ for narrow dispersity materials with similar compositions.[39] Some similar phenomena were also reported in poly(ethylene oxide-*b*-1,4-butadiene-*b*-ethylene oxide) (OBO) copolymers, in which narrow dispersity O blocks flank a broad dispersity center B block.[37] Matsen's recent self-consistent mean-field theory analyses of these polydisperse ABA triblock copolymer systems semiquantitatively predict the observed shifts in the composition-dependent phase windows, yet the theoretically anticipated domain spacings are much smaller than those observed experimentally.[40] Thus, segmental dispersity provides a new means for controlling block copolymer morphology and microphase-separated melt stability.

The phenomenology of broad dispersity block copolymer phase behavior has been rationalized in terms of two synergistic effects, arising from the segmental molecular weight dispersity and consequent composition dispersity of these samples.[32,39,41] While the relative contributions of these effects are thought to depend on the segmental incompatibility quantified by χ_{AB}, few studies have systematically investigated the effects of segmental dispersity in strongly segregated copolymers. Given that multifunctional block copolymer materials for ion transport, water filtration, and other advanced technologies may naturally rely on broad dispersity, high χ_{AB} block copolymers, one must understand the effects of large segmental interaction parameters on the phase behavior of these useful yet polydisperse materials.

Herein, we report initial studies of the effects of center B block dispersity in strongly segregated poly(lactide-*b*-1,4-butadiene-*b*-lactide) (LBL) triblock copolymers, derived from tandem chain transfer ring-opening metathesis polymerization (ROMP-CT) and ring-opening transesterification polymerization (ROTEP). Using two different approaches, we quantify the segmental interaction parameter χ_{LB} between the L and B blocks and show that it is 6 times larger than that of previously studied polydisperse SBS[38] and OBO[37] triblock copolymer systems. While Pitet and Hillmyer recently reported the mechanical properties of higher molecular weight LBL copolymers derived from a conceptually similar synthetic route, quantitative comparisons of the melt phase behaviors of these polydisperse copolymers and their narrow dispersity analogues have not been previously reported.[42] We use temperature-dependent synchrotron SAXS to demonstrate that the lamellar phase composition window for broad dispersity copolymers shifts to asymmetric volume fractions, in a manner consistent with previous reports. However, the lamellar domain spacings are much smaller than expected based on previous studies of polydisperse copolymer melts. Furthermore, the molecular-weight-dependent domain spacing scaling relationship is unexpectedly similar to that of narrow dispersity LBL triblock copolymers.

EXPERIMENTAL METHODS

Materials. All reagents were purchased from Sigma-Aldrich Chemical Co. (Milwaukee, WI) and used without further purification, unless specifically noted below. *trans,trans,cis*-1,5,9-Cyclododecatriene (CDT) was distilled prior to use, and *cis*-1,4-diacetoxy-2-butene was distilled from CaH_2. Lactide was recrystallized from ethyl acetate, thoroughly vacuum-dried, and stored under an inert atmosphere. 1,8-Diazabicyclo[5.4.0]undec-7-ene (DBU) was vacuum distilled from CaH_2 and stored under an inert atmosphere. 1,3-Butadiene was doubly distilled from dry *n*BuLi immediately prior to use, while ethylene oxide was doubly distilled from dry *n*BuMgCl prior to use. Anhydrous and anaerobic toluene and cyclohexane were obtained by sparging analytical grade solvents with N_2(g) for 30 min followed by cycling through a column of activated neutral alumina in a Vacuum Atmospheres solvent purification unit. 3-Tri(isopropyl)-siloxypropyllithium (TIPSO-PrLi) in cyclohexane ([TIPSO-PrLi] = 0.49 M) was synthesized according Meuler et al.[43] and stored under N_2(g) at −32 °C prior to use. A narrow dispersity telechelic α,ω-dihydroxypoly(1,4-butadiene) with $M_{n,SEC} = 10.0$ kg/mol and $Đ = 1.06$ (versus PB Standards) was synthesized per a previously reported procedure using TIPSO-PrLi.[37]

^{1}H NMR Characterization. Copolymer compositions were determined from quantitative ^{1}H NMR spectra recorded on a Bruker AC+ 300 spectrometer and referenced to added tetramethylsilane ($(CH_3)_4Si$). All spectra were acquired using a pulse repetition delay of 10 s in order to ensure quantitatively accurate peak integrations.

Size-Exclusion Chromatography (SEC). SEC analyses were performed using a Viscotek GPCMax system equipped with two Polymer Laboratories Resipore columns (250 mm × 4.6 mm), and four Viscotek detectors, including a differential refractometer, two angle-light scattering detector (7° and 90°), and a four capillary differential viscometer. THF was used as the mobile phase at 40 °C with a 0.8 mL/min flow rate. M_n and $Đ = M_w/M_n$ for each PB macroinitiator were determined using a calibration curve constructed by Mark−Houwink correction of a polystyrene (PS) calibration curve to poly(1,4-butadiene).[44] The PS calibration curve was constructed using narrow molecular weight standards with $M_n = 580-377400$ kg/mol (Polymer Laboratories, Amherst, MA). M_n for PLA homopolymers was determined using a poly(styrene) calibration curve that was similarly corrected using the known Mark−Houwink values.[45] Values of $Đ$ for LB diblock and LBL triblock copolymers are reported against PS standards without correction.

Small-Angle X-ray Scattering (SAXS). Laboratory SAXS measurements employed a Rigaku SMAX-300 High Brilliance instrument, using Cu Kα X-rays generated by a Rigaku Micromax 002+ source that were collimated with a Max-Flux multilayer confocal optic and three pinholes to furnish a final beam diameter ≤0.5 mm. Samples were mounted on a Linkam hot stage in a vacuum chamber

dx.doi.org/10.1021/ma5006233 | *Macromolecules* 2014, 47, 4346−4356

Table 1. Molecular Parameters of Narrow Dispersity LB Diblock Copolymers

sample	$M_{n,B}$ [a]	$Đ_B$ [a]	$M_{n,L}$ [b]	$M_{n,total}$ [b]	$Đ_{total}$ [c]	f_B [d]	N [e]	$\chi_{LB}N$ [f]	q^* [g] (Å^{-1})	d [g] (nm)	morphology [g]
mLB-3.4-52	1.5	1.08	1.9	3.4	1.08	0.52	46	8.9	0.0705		DIS
mLB-4.0-54	1.8	1.08	2.2	4.0	1.08	0.54	55	10.5	0.0656	9.6	LAM [i]
mLB-5.6-49	2.3	1.07	3.3	5.6	1.08	0.49	77	14.7	0.0504 [h]	12.5 [h]	LAM [h]

[a] Determined by size exclusion chromatography (SEC) in THF at 40 °C against Mark–Houwink corrected PS calibration standards for PB. [b] Calculated from quantitative ^{1}H NMR spectra using $M_{n,B}$. [c] Determined using SEC in THF at 40 °C against PS calibration standards. [d] Calculated using the homopolymer melt densities ρ_{PB} = 0.826 g/mL[55] and ρ_{PLA} = 1.154 g/mL at 140 °C.[56] [e] Calculated using a 118 Å^3 reference volume. [f] Calculated at 155 °C using χ_{LB} = 0.1924. [g] Determined from synchrotron SAXS at 140 °C. [h] Determined from synchrotron SAXS at 120 °C. [i] This sample exhibits an order-to-disorder transition at 155 °C.

and thermally equilibrated for 10 min at each temperature prior to data acquisition; typical X-ray exposure times were ~3–5 min. 2D-SAXS patterns were recorded on a Gabriel X-ray detector (12 cm diameter active area) at a sample-to-detector distance of either 1 or 2 m. The precise sample-to-detector distance was calibrated using a silver behenate standard (d = 58.38 Å).

Synchrotron SAXS measurements were performed at the 5-ID-D beamline of the DuPont–Northwestern–Dow Collaborative Access Team (DND-CAT) at the Advanced Photon Source (Argonne, IL). Experiments employed a beam energy of 17 keV (λ = 0.7293 Å^{-1}) and sample-to-detector distances of 3.067 or 2.979 m. 2D-SAXS patterns were recorded on a MAR-CCD detector (133 mm diameter active circular area) with 2048 × 2048 pixel resolution. Samples were thermostated at the desired temperature in a Linkam DSC X-ray stage and allowed to equilibrate for 5 min prior to data collection (typical exposure times ~2 s). Data reduction was performed using freely available Igor Procedures files developed by Schmitt et al.[46]

Transmission Electron Microscopy (TEM). Copolymer monoliths were cryo-sectioned at −120 °C, using a Leica UltraMicrotome to yield flat samples with thicknesses ~80–100 nm. Sections were transferred to Cu grids (400 mesh) and exposed to the vapor over a 4 wt % OsO_4(aq) solution for 1 h, which selectively stained the unsaturated poly(1,4-buadiene) segments for enhanced imaging contrast. Within 24 h of staining, samples were imaged at ambient temperature using a LEO 912 EFTEM operating at an accelerating voltage of 120 keV.

Representative Synthesis of Broad Dispersity α,ω-Dihydroxypoly(1,4-butadiene). CDT (10.00 g, 61.63 mmol), 1,4-diacetoxy-2-butene (0.1076 g, 0.625 mmol), and toluene (20 mL) were combined in a dry 100 mL Schlenk flask. In degassing this solution by three freeze–thaw cycles, Grubbs' second-generation olefin metathesis catalyst (6 mg, 7.07 μmol) was added during the final freezing cycle, and the flask was evacuated and purged with N_2(g) three times prior to thawing under vacuum. After stirring for 48 h at 22 °C, the reaction was quenched with ethyl vinyl ether (1 mL) and stirred for 30 min. CH_2Cl_2 (20 mL) was added to reduce the solution viscosity, and the resulting α,ω-diacetoxypoly(1,4-butadiene) was isolated by precipitation into CH_3OH and subsequent vacuum filtration of the solids. Quantitative ^{1}H NMR end-group analysis using the relative peak areas of the allylic acetoxy end groups ($-CH_2OC(O)CH_3$) and the olefinic backbone ($=CH-CH_2-$) were used to determine $M_{n,NMR}$ = 16.6 kg/mol. $M_{n,SEC}$ = 17.8 kg/mol and $Đ$ = 1.72 (using Mark–Houwink corrected SEC for poly(1,4-butadiene)).

α,ω-Diacetoxypoly(1,4-butadiene) (~10 g, 0.563 mmol) was dissolved in THF (150 mL) and stirred with excess $KOCH_2CH_3$ (0.189 g, 2.25 mmol, 2 equiv per chain end) at 22 °C for 1 h to deprotect the hydroxyl end groups. The solvent was removed via rotary evaporation, and the resulting solid was subsequently redissolved in CH_2Cl_2 and precipitated into CH_3OH. The collected polymer was freeze-dried from C_6H_6. $M_{n,SEC}$ = 17.7 kg/mol (from Mark–Houwink corrected SEC) and $Đ$ = 1.76 (versus PB standards).

Representative Synthesis of Narrow Dispersity α-Hydroxypoly(1,4-butadiene). A narrow dispersity, semitelechelic α-hydroxypoly(1,4-butadiene) was synthesized by anionic polymerization by analogy to a previously reported procedure.[43] A 1 L five-port reactor under N_2(g) charged with anhydrous cyclohexane (500 mL) was thermostated at 40 °C, and TIPSO-PrLi (8.3 mL, 0.49 M solution in cyclohexane) was added via an airtight syringe. 1,3-Butadiene (7.734 g, 0.1430 mol) was slowly added to maintain a nearly constant reactor pressure of 6–10 psig, and the reaction was stirred for 16 h. The reaction was quenched by injection of HCl/MeOH (1.64 mL 12.4 M HCl(aq) in 10 mL of MeOH) and stirred for 30 min, prior to exposure to air. After removal of the volatile solvents by rotary evaporation, the resulting polymer was isolated by redissolution in CH_2Cl_2 (100 mL) and extraction with saturated $NaHCO_3$(aq) (2 × 100 mL), and deionized H_2O (100 mL), followed by rotary evaporation. The polymer was then dissolved in THF (150 mL), and a 5-fold excess of Bu_4NF (7.94 g 75 wt % solution in H_2O, 0.0228 mol) was added. This reaction mixture was stirred for 48 h to quantitatively cleave the TIPS protecting group. The reaction solvent was removed under reduced pressure, and the resulting polymer was dissolved in CH_2Cl_2 (100 mL) and washed with H_2O (3 × 100 mL). Evaporation of the solvent under reduced pressure yielded a polymeric liquid, which was dried azeotropically by repeated coevaporations with C_6H_6 (3 × 30 mL). ^{1}H NMR reveals that the polymer contains 93% 1,4-addition and 7% 1,2-addition of butadiene monomer units. $M_{n,NMR}$ = 1.8 kg/mol from quantitative ^{1}H NMR end-group analysis using the allylic end groups ($=CH-CH_2-OH$) and the olefinic backbone ($=CH-CH_2-$) resonances. $M_{n,SEC}$ = 2.0 kg/mol and $Đ$ = 1.08 (versus PB Standards from Mark–Houwink corrected SEC). $M_{n,NMR}$ was used in all subsequent analysis.

Representative Synthesis of LBL Block Copolymers. Telechelic PB macroinitiator ($M_{n,SEC}$ = 17.7 kg/mol, $Đ$ = 1.76, 0.539 g, 30.5 μmol) and lactide monomer (0.465 g, 3.20 mmol) were added to a 20 mL vial and stirred with dry, degassed toluene (15 mL). This mixture was stirred for >1 h to create a fine dispersion of lactide. Chain extension block copolymerization was initiated by the addition of DBU (0.697 mL of 0.046 M DBU in toluene), followed by stirring for 2 h at 22 °C according to the protocol of Lohmeijer et al.[47] The reaction was quenched with benzoic acid (1.00 mL of 0.164 M benzoic acid in toluene) and stirred for 30 min. The resulting polymers were coagulated by slow precipitation into cold CH_3OH (0 °C), collected by filtration, and dried *in vacuo*. Multiple polymerizations were performed in parallel by changing the relative weight fractions of PB and lactide monomer, while maintaining [lactide]:[DBU] = 100:1. Molecular weight analyses from SEC and quantitative ^{1}H NMR composition analyses of the resulting copolymers are provided in Table 2. We adopt the nomenclature LBL-*xx*-*yy*, whereby *xx* denotes the overall molecular weight of the triblock copolymer in kg/mol and *yy* indicates the volume fraction f_B.

Narrow dispersity mLB diblock and mLBL triblock copolymers were synthesized in a similar parallel fashion. In order to prevent polymer cross-linking during temperature-dependent analyses of these samples, these copolymers were freeze-dried from C_6H_6 containing 0.5 wt % Irganox 1076 as a stabilizer. The molecular characterization information for narrow dispersity mLB diblock and mLBL triblock copolymers is furnished in Tables 1 and 2, respectively.

Cross-Metathesis Degradation of LBL Triblock Copolymers.[48] LBL-27.9-56 (150 mg), 1-hexene (2 mL), and benzene (2 mL) were combined in a 100 mL Schlenk flask and degassed by three freeze–thaw cycles. During the last freezing cycle, Grubbs' second-generation olefin metathesis catalyst (6 mg, 7 μmol) was added, and the flask was evacuated and refilled with N_2(g) three times. Metathesis

dx.doi.org/10.1021/ma5006233 | Macromolecules 2014, 47, 4346–4356

degradation commenced upon warming the flask to 22 °C. After 48 h, the reaction was quenched with ethyl vinyl ether (1 mL), and the solution was precipitated into cold CH_3OH (15 mL). The isolated polymer was freeze-dried from C_6H_6. ^1H NMR confirms complete removal of the poly(1,4-butadiene) segment. $M_{n,SEC}$ = 7.9 kg/mol (versus PLa Standards) ($M_{n,thy}$ = 7.3 kg/mol from quantitative ^1H NMR analysis) and $Đ$ = 1.10 (versus PS Standards).

RESULTS AND ANALYSIS

Determination of χ_{LB}. In order to investigate how the magnitude of χ_{AB} affects the location of the composition-dependent phase window and the domain spacings of the lamellar mesophases adopted by polydisperse ABA triblock copolymers, we sought to design a model copolymer system with a larger segmental interaction parameter χ_{AB} than the previously reported SBS and OBO triblock copolymers (S = poly(styrene), B = poly(1,4-butadiene), and O = poly(ethylene oxide)). Using Hildebrand's solubility parameter formalism in conjuction with concepts in regular solution theory,[49] one can express χ_{AB} for any polymer pair as

$$\chi_{AB} = \frac{v}{kT}(\delta_A - \delta_B)^2$$

wherein v = 118 Å^3 is an arbitrarily chosen reference volume, k is the Boltzmann constant, T is the absolute temperature, and δ_i is the solubility parameter for homopolymer i. Given the previously determined expressions $\chi_{SB}(T) = (30.137/T) - 0.03813$,[38] δ_S = 19.51 (MPa)$^{1/2}$,[44] δ_B = 17.73 (MPa)$^{1/2}$,[44] δ_L = 21.07 (MPa)$^{1/2}$,[50] and the fact that

$$\frac{\chi_{LB}}{\chi_{SB}} = \frac{(\delta_L - \delta_B)^2}{(\delta_S - \delta_B)^2}$$

we estimate that χ_{LB} = 0.1137 at 155 °C. We note that χ_{LB} determined from this formalism likely underestimates the actual value of the interaction parameter between poly(lactide) and 100% regioregular poly(1,4-butadiene), since the values of $\chi_{SB}(T)$ and the solubility parameter δ_B are associated with poly(1,4-butadienes) produced from anionic polymerizations. The latter polymers typically contain 7% of the 1,2-regioisomer and 93% of the 1,4-regioisomer, whereas the polymers used in this study comprise 100% of the 1,4-regioisomer.[38] Thus, χ_{LB} appears significantly larger than χ_{SB} and χ_{OB} as desired.

To determine the magnitude of χ_{LB} more precisely, we synthesized a series of narrow dispersity, symmetric composition mLB diblock copolymers and measured the molecular weight dependence of their order−disorder transition temperatures (T_{ODT}).[51−53] By measuring the dependence of T_{ODT} on the segment density normalized degree of polymerization (N) of an mLB diblock copolymer in combination with the mean-field theory result $(\chi_{LB}N)_{ODT}$ = 10.5,[4] we sought to determine the temperature-dependent $\chi_{LB}(T) = (A/T) + B$. Three narrow dispersity LB diblock copolymers were synthesized by tandem anionic polymerizations of 1,3-butadiene followed by DBU-catalyzed organocatalytic ROTEP of lactide[47] (Scheme 1). The molecular parameters of these samples are given in Table 1. We found that nearly symmetric, narrow dispersity mLB-4.0−0.54 diblock copolymer with M_n = 4.0 kg/mol ($Đ$ = 1.08) exhibits a lamellar morphology with T_{ODT} = 155 °C (Figure 1), as determined by synchrotron SAXS. Neglecting fluctuation effects,[54] mean-field theory analysis of this copolymer sample yields χ_{LB} = 0.1924 at 155 °C. From the molecular parameters of the mLB diblock copolymers provided in Table 1, we note that the lack of accessible order−disorder transition temperature for mLB-5.6-49 implies that T_{ODT} depends strongly on N for these LB diblocks. This strong N dependence and weak temperature dependence precluded the intended determination of $\chi_{LB}(T)$. These observations corroborate our initial solubility parameter analysis, which predicts a relatively large value for χ_{LB}.

Scheme 1. Synthesis of Narrow Dispersity mLB Diblock Copolymers by Tandem Anionic and Ring-Opening Transesterification Polymerizations

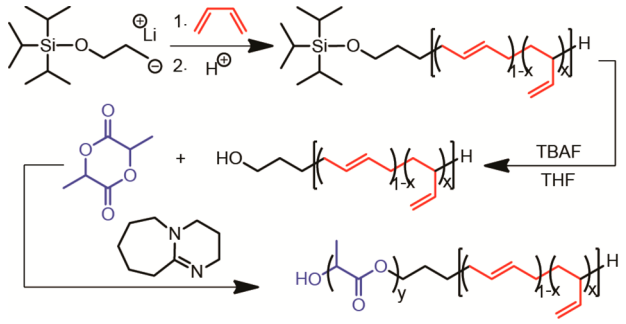

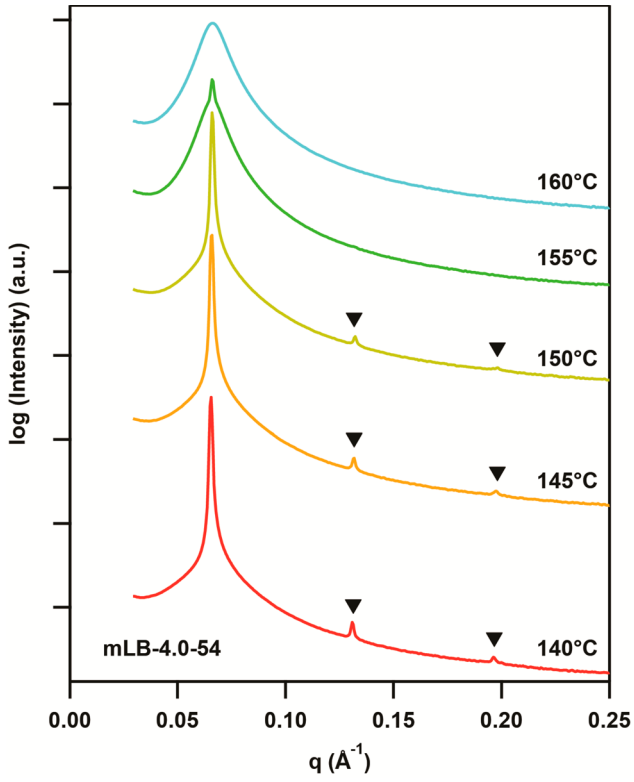

Figure 1. Azimuthally-integrated, temperature-dependent SAXS patterns for mLB-4.0-54, demonstrating the formation of a lamellar morphology with q^* = 0.0656 Å^{-1} (d = 9.59 nm). The order−disorder transition temperature T_{ODT} = 155 °C was identified by the disappearance of the higher order scattering maxima ($2q^*$ and $3q^*$ as indicated by markers) and the appearance of the low intensity correlation-hole scattering peak associated with a disordered copolymer melt.

Another established method for determining $\chi_{LB}(T)$ relies on fitting the temperature-dependent correlation-hole scattering peak shape and intensity for a disordered LB diblock copolymer using the random phase approximation.[4,51] We performed this analysis using the disordered state scattering profiles for mLB-4.0-54 at 160 and 170 °C (see Supporting Information for

dx.doi.org/10.1021/ma5006233 | Macromolecules 2014, 47, 4346−4356

details of this analysis). We deduced that χ_{LB} = 0.177 at 160 and 170 °C from this approach, affirming the weak temperature dependence of χ_{LB}. We note that this value of χ_{LB} is only 8% lower than the value derived from the T_{ODT} measurement for this same diblock copolymer.

Lee et al. recently determined the dependence of T_{ODT} on the degree of polymerization N for a series of symmetric LBL triblock copolymers, and they combined this data with the triblock copolymer mean-field result $(\chi_{LB}N)_{ODT}$ = 17.9 (neglecting fluctuation effects) to obtain $\chi_{LB}(T) = 161.6/T - 0.223$.[57] This expression yields χ_{LB} = 0.154 at 155 °C, which is ~20% lower than the value we estimate from our measurements of T_{ODT} for mLB-3.94-54. Given the caveats associated with each of the above methods for determining $\chi_{LB}(T)$, the relative consistency of the three obtained values is remarkable. Since the values derived from SAXS analyses rely on mean-field theory, these values neglect the role of fluctuation effects that are substantial at low degrees of polymerization N considered here. In view of this last point, our value χ_{LB} = 0.1924 at a reference temperature of 155 °C is an underestimate of the actual value of the $\chi_{LB}(T)$. In the remainder of this paper, we use the last value in reporting the segregation strengths associated with our LBL triblock copolymers.

Combinatorial Synthesis of LBL Triblock Copolymers. We combinatorially synthesized a series of broad dispersity LBL triblock copolymers using tandem ROMP-CT and organocatalytic ROTEP (Scheme 2). ROMP-CT of 1,5,9-cyclododecatriene (CDT) in the presence of the acyclic olefin chain transfer agent 1,4-diacetoxy-2-butene (CTA) catalyzed by Grubbs' second-generation olefin metathesis catalyst (GII) yields α,ω-diacetoxy poly(1,4-butadiene) with a theoretical molecular weight $M_{n,thy}$ = [CDT]/[CTA] and a most probable distribution of molecular weights.[58] These polymerizations are known to furnish α,ω-telechelic homopolymers with a high degree of chain end functionality (F_n = 2.0), if [CTA]/[GII] ≥ 100:1. Using these reaction conditions, we obtained a series of α,ω-diacetoxypoly(1,4-butadienes) with M_n = 4.5−17.7 kg/mol and $Đ$ = 1.72−1.88. The close agreement between $M_{n,thy}$ and $M_{n,NMR}$ from quantitative ^{1}H NMR end-group analysis and $M_{n,SEC}$ within ~10% indicates the expected high degree of chain end functionality (F_n = 2.0) for these telechelic, "perfectly linear" poly(1,4-butadienes). Subsequent saponification of the acetate ester end groups with $KOCH_2CH_3$ yields α,ω-dihydroxypoly(1,4-butadienes) ($PB(OH)_2$). On the basis of a report by Lohmeijer et al.,[47] we initiated the organocatalytic ROTEP of lactide catalyzed by DBU from these α,ω-telechelic $PB(OH)_2$ homopolymers to obtain the desired LBL triblock copolymers with f_B = 0.44−0.79 and $M_{n,total}$ = 12.4−28.7 kg/mol. An important feature of our optimized organocatalytic ROTEP of lactide is that it enables the straightforward synthesis of a series of LBL triblock copolymers with well-defined target compositions, by controlling the relative amounts of the $PB(OH)_2$ macroinitiator and lactide monomer added to each polymerization mixture due to the fact that these chain extension reactions may be run to 100% lactide monomer conversion. Consequently, we synthesized 13 LBL triblock copolymers in parallel fashion to produce a modest sample library in only a few days (Table 2).

Scheme 2. Tandem ROMP-ROTEP Synthesis of Broad Dispersity LBL Triblock Copolymers

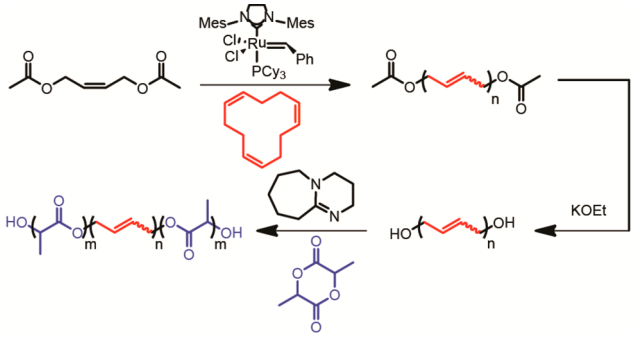

We note that Pitet and Hillmyer previously reported the syntheses of related polydisperse LBL block copolymers using tandem ROMP-CT and alkylaluminum-catalyzed lactide ROTEP,[42] as part of their studies of the mechanical properties of these thermoplastic elastomers. However, their syntheses employed unpurified 1,5-cyclooctadiene in the ROMP-CT of the α,ω-dihydroxy poly(1,4-butadienes). Due to the presence of the acyclic olefin 4-vinylcyclohexene as an impurity in their 1,5-cyclooctadiene,[59] their $PB(OH)_2$ macroinitiators had only a modest chain end degree of functionalization F_n ~ 1.5. ROTEP chain extension block copolymerization of lactide using these $PB(OH)_2$ macroinitiators thus results in the formation of ill-defined mixtures of broad dispersity LB diblock and LBL triblock copolymers. This synthetic complexity precludes the use of their data in definitively identifying the effects of B segment dispersity on the locations of the composition-dependent morphology windows in LBL triblock copolymers and the lamellar domain spacing scaling relationships.

One significant advantage of our model LBL triblock copolymer system is that we are able to quantitatively and independently characterize the M_n and $Đ$ of each of the constituent blocks of each copolymer sample. The final copolymer composition and M_n of the L block were determined from quantitative ^{1}H NMR, by comparison of the allylic resonances of PB ($-CH_2-CH=$) with the methyl resonances of L block ($-(C=O)-CH(CH_3)-O-$). In order to assess the molar mass dispersity of the L block derived from organocatalytic lactide ROTEP, a subset of the broad dispersity LBL triblocks were subjected to cross metathesis degradation against 1-hexene in C_6H_6 catalyzed by GII by analogy to previous reports.[48] The L homopolymers arising from these degradation reactions were analyzed using SEC and found to have $M_{n,L}$ values in agreement with those deduced from ^{1}H NMR analysis of the triblock copolymers based on the B block M_n ($M_{n,L,NMR}$ = 7.3 kDa and $M_{n,L,SEC}$ = 7.9 kDa using Mark−Houwink corrected calibration curve). SEC analyses establish that the L block dispersities are narrow, typically $Đ$ = 1.10−1.20 (see Table 2 and Supporting Information Figure S1).

LBL Lamellar Phase Composition Window. Given that χ_{LB} = 0.192 at 155 °C is an underestimate of the true value of the interaction parameter (*vide surpra*), the molecular parameters of the LBL triblocks listed in Table 2 imply that these copolymer melts are strongly segregated as $\chi_{LB}N$ = 35.1−83.6.[7−9] Each of the LBL triblock copolymers listed in Table 2 was subjected to temperature-dependent synchrotron SAXS analysis, in order to identify its equilibrium microphase-separated morphology and associated microdomain spacing (d). SAXS patterns for each of these samples exhibit scattering maxima at q^*, $2q^*$, $3q^*$, and $4q^*$ that correspond to the (100), (200), (300), and (400) scattering reflections of a lamellar mesophase (Figure 2). LBL-14.9-52 displays a strong primary scattering peak at q^* = 0.0432 Å^{-1}($d = 2\pi/q^*$ = 14.6 nm),

dx.doi.org/10.1021/ma5006233 | Macromolecules 2014, 47, 4346−4356

Table 2. Broad and Narrow Dispersity LBL Triblock Copolymers

sample	$M_{n,B}$ [a]	$Đ_B$ [a]	$M_{n,L}$ [b]	$Đ_L$ [c]	$M_{n,total}$ [b]	$Đ_{total}$ [c]	f_B [d]	N [e]	morphology [f]
LBL-12.5-44	4.5	1.88	4.0		12.5	1.18	0.44	175	CYL
LBL-14.9-52	6.6	1.73	4.2	1.12	14.9	1.35	0.52	214	LAM
LBL-17.8-53	7.9	1.88	5.0	1.20	17.8	1.35	0.53	255	LAM
LBL-27.9-56	13.3	1.72	7.3	1.10	27.9	1.32	0.56	404	LAM
LBL-13.4-57	6.6	1.73	3.4		13.4	1.25	0.57	195	LAM
LBL-15.0-61	7.9	1.88	3.6		15.0	1.43	0.61	221	LAM
LBL-12.4-61	6.6	1.73	2.9		12.4	1.27	0.61	183	LAM
LBL-14.7-62	7.9	1.88	3.4		14.7	1.42	0.62	218	LAM
LBL-23.9-64	13.3	1.72	5.3	1.10	23.9	1.37	0.64	355	LAM
LBL-28.7-69	17.7	1.76	5.5		28.7	1.48	0.69	435	LAM
LBL-20.0-73	13.3	1.72	3.4		20.0	1.44	0.73	309	LAM
LBL-25.8-75	17.7	1.76	4.1		25.8	1.50	0.75	400	LAM
LBL-18.2-79	13.3	1.72	2.5		18.2	1.49	0.79	286	DIS CYL
mLBL-43.2-30	10.0	1.06	16.6		43.2	1.06	0.30	373	CYL
mLBL-33.6-37	10.0	1.06	11.8		33.6	1.07	0.37	314	LAM
mLBL-25.3-48	10.0	1.06	7.6		25.3	1.07	0.48	264	LAM
mLBL-23.4-51	10.0	1.06	6.7		23.4	1.07	0.51	252	LAM
mLBL-21.4-55	10.0	1.06	5.7		21.4	1.06	0.55	240	LAM
mLBL-19.8-59	10.0	1.06	4.9		19.8	1.06	0.59	230	LAM
mLBL-17.9-64	10.0	1.06	3.9		17.9	1.06	0.64	218	LAM
mLBL-17.8-64	10.0	1.06	3.9		17.8	1.05	0.64	218	LAM
mLBL-14.7-75	10.0	1.06	2.3		14.7	1.06	0.75	199	CYL

[a]Determined by size exclusion chromatography (SEC) in THF at 40 °C against Mark−Houwink corrected PS calibration standards for PB. [b]Calculated from quantitative ^{1}H NMR spectra using $M_{n,B}$. [c]Determined using SEC in THF at 40 °C against PS calibration standards. [d]Calculated using the homopolymer melt densities ρ_{PB} = 0.826 g/mL[55] and ρ_{PLA} = 1.154 g/mL[56] at 140 °C. [e]Calculated using a 118 Å^3 reference volume. [f]Determined by synchrotron small-angle X-ray scattering (SAXS) at 120 °C.

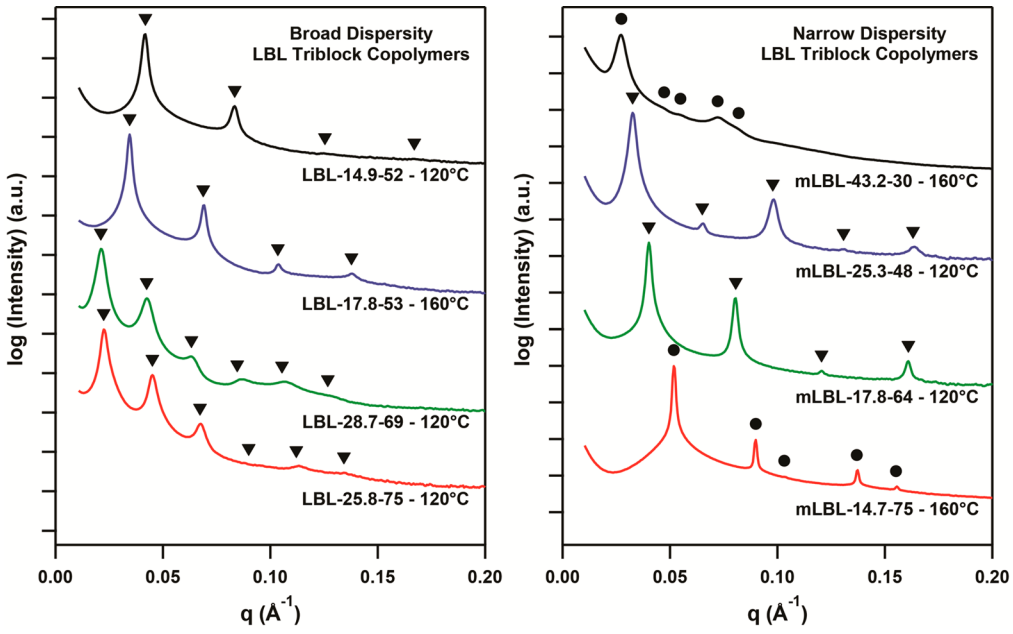

Figure 2. Azimuthally-integrated SAXS patterns for broad dispersity (*left*) and narrow dispersity (*right*) LBL triblock copolymers. Broad dispersity LBL samples (*left*) exhibit scattering maxima characteristic of lamellar mesophases with peaks at q^*, $2q^*$, $3q^*$, and $4q^*$ and in some cases $5q^*$ and $6q^*$ as indicated by the triangular markers. Narrow dispersity LBL control samples (*right*) instead exhibit lamellar and cylindrical morphologies (scattering maxima at q^*,$\sqrt{3}q^*$,$\sqrt{4}q^*$,$\sqrt{7}q^*$, and $\sqrt{9}q^*$ as indicated by the circular markers), depending on the copolymer composition.

along with an intense peak located at $2q^*$. The weak higher order $3q^*$ and $4q^*$ peaks indicate a low degree of translational order, which we attribute to slight deviations in the lamellar microdomain spacing arising from the proximity of this sample composition to the lamellae/cylinder phase boundary (*vide infra*). Increasing the B composition and overall copolymer M_n slightly as in LBL-17.8-53 results in better long-range, microphase-separated order, as evidenced by the appearance of four SAXS maxima with significantly sharper peaks with smaller full widths at half-maximum. The increased molecular weight of this sample results a lamellar morphology with a slightly larger domain spacing d = 18.2 nm. SAXS patterns of

dx.doi.org/10.1021/ma5006233 | *Macromolecules* 2014, 47, 4346−4356

the compositionally asymmetric polymer sample LBL-28.7-69 exhibit six SAXS peaks, suggestive of exceptional long-range lamellar order with a primary scattering peak located at q^* = 0.0213 Å^{-1} (d = 29.5 nm). These scattering analyses demonstrate that B segment dispersity in these strongly segregated block copolymer melts does not significantly perturb the periodic, long-range order in these lamellar block copolymer mesophases. Notably, broad dispersity LBL triblocks with f_B = 0.44 and 0.79 exhibit SAXS patterns consistent with cylindrical morphologies (see Supporting Information Figure S2). On the basis of the observation of these nonlamellar morphologies, we conclude that the lamellar mesophase is stable when $0.52 \leq f_B \leq 0.75$ for broad dispersity LBL copolymers.

We verified the morphological assignments from SAXS by transmission electron microscopy (TEM) imaging of select LBL triblock copolymer samples (Figure 3). Samples were

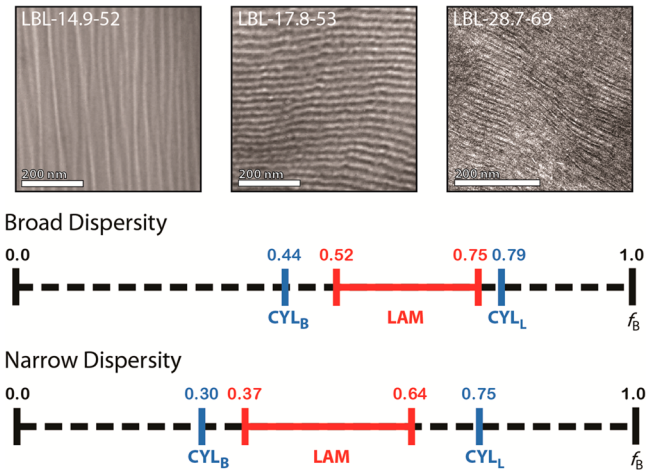

Figure 3. Representative TEM images of lamellar morphologies formed by LBL-14.9-52, LBL-17.8-53, and LBL-28.7-69, in which the B domains have been stained with OsO_4 for enhanced imaging contrast (*top*). The unusual texture for sample LBL-28.7-69 (alternating thick and thin stripes) arises from B block crystallization near the centers of the microdomains, which inhibits stain permeation throughout the entire B domain. A graphical depiction of the experimentally determined positions of the lamellar mesophase composition windows for broad and narrow dispersity LBL triblock copolymers (*bottom*).

cryo-sectioned at −120 °C, and the B segments were selectively stained using OsO_4 vapor prior to imaging. Each sample exhibits a lamellar microdomain structure, albeit with subtle differences. Consistent with the above SAXS analyses, images of LBL-14.9-52 exhibit a low degree of long-range translational order accompanied by variations in the lamellar domain thickness. On the other hand, LBL-17.8-53 exhibits well-ordered lamellar domains that are also consistent with the above SAXS data. TEM images of LBL-28.7-69 display the apparent formation of a lamellar domain structure with alternating thick and thin stripes having diffuse and sharp interfaces, respectively. We ascribe this unusual texture to the semicrystalline nature of the B segments[60] under the conditions used for TEM sample preparation, which prevents the permeation of the OsO_4 throughout the B domains. Consequently, the minority L domains (f_L = 0.31) appear as thin, white stripes and the B domains appear as thicker gray stripes with dark outlines due to the concentration of the metallic stain near the domain interfaces at which the B segments are amorphous. Hence, the TEM analyses confirm that the lamellar mesophase composition window for our polydisperse LBL triblock copolymers spans the volume fraction range f_B = 0.52−0.75, albeit with varying degrees of long-range nanoscale order.

To determine directly the extent to which midblock dispersity shifts of the composition-dependent lamellar phase window, we used synchrotron SAXS to study the phase behavior of a series of narrow dispersity mLBL triblock copolymers derived from organocatalytic ROTEP of lactide initiated from a narrow dispersity α,ω-hydroxypoly(1,4-butadiene) with $M_{n,B}$ = 10.0 kg/mol. mLBL-25.3-48 exhibits high-intensity SAXS peaks consistent with a lamellar mesophase with near symmetric volume fraction (expected $\sqrt{4}q^*$ and $\sqrt{16}q^*$ extinctions) with q^* = 0.0326 Å^{-1} (d = 19.3 nm) (Figure 2, right). SAXS patterns for mLBL-17.8-64 also correspond to a lamellar mesophase with a volume fraction near f_B = 2/3, as evidenced by the $\sqrt{9}q^*$ extinction (q^* = 0.0402 Å^{-1}, d = 15.6 nm). However, mLBL-43.2-30 instead exhibits scattering maxima at q^*, $\sqrt{3}q^*$, $\sqrt{4}q^*$, $\sqrt{7}q^*$, and $\sqrt{9}q^*$, consistent with a hexagonally packed cylinders morphology. SAXS patterns for mLBL-14.7-75 also display scattering maxima corresponding to a cylinders morphology with a $\sqrt{4}q^*$ extinction. Thus, these samples bracket the lamellar phase composition window for narrow dispersity LBL copolymers (Figure 3) in the range f_B = 0.37−0.64.

A graphical comparison of the copolymer composition windows over which lamellar phases form in broad and narrow dispersity LBL triblock copolymers is provided in Figure 3. From this diagram, we conclude that the lamellar phase window in the broad dispersity samples is substantially shifted toward higher volume fractions f_B of the polydisperse segment. While this result may initially seem surprising, this shift in the composition-dependent phase window is consistent with our previous reports on SBS[39] and OBO[37] triblock copolymers with broad dispersity center B blocks ($Đ$ = 1.70−2.00).

Lamellar Domain Spacing (d) Scaling. The characteristic length scale associated with a narrow dispersity A/B block copolymer ordering into a lamellar mesophase depends sensitively on the overall segment density-normalized degree of polymerization (N) and the interaction parameter χ_{AB}. These functional dependences are respectively related to the overall chain dimensions and the extent to which the chains stretch to mitigate enthalpically unfavorable A/B monomer contacts. Theoretical approaches predict that the microdomain spacings (d) scale as $d \propto N^{\beta}$. In weakly segregated and disordered melts, β = 1/2 as expected for the radius of gyration of a polymeric random walk.[7] Strong segregation theories for AB diblock and ABA triblock copolymers predict that β = 2/3,[10] which is close to that found in experimental studies.[14] In the strong segregation limit, symmetric ABA triblock copolymers with a degree of polymerization N are experimentally observed to exhibit d-spacings that are ∼10% greater than those of symmetric AB diblock copolymers of length (N/2).[13]

The β-values for broad dispersity diblock and multiblock copolymer lamellar mesophases have yet to be quantitatively determined. Table 3 lists the d-spacings associated with our broad dispersity LBL triblock copolymers derived from SAXS analyses at 120 °C along with those for the narrow dispersity mLBL analogues. From these data, we immediately note that the d-spacings for the broad dispersity LBL copolymers are greater than those of the mLBL samples at similar total

dx.doi.org/10.1021/ma5006233 | *Macromolecules* 2014, 47, 4346−4356

Table 3. Experimental and Theoretical Lamellar *d*-Spacings for Broad and Narrow Dispersity LBL Triblock Copolymers

sample	$\chi_{LB}N^a$	$q^{*\,b}$ (Å^{-1})	$d_{expt}{}^c$ (nm)	$d_{thy}{}^d$ (nm)
LBL-14.9-52	41.2	0.0395	15.9	15.4
LBL-17.8-53	49.1	0.0275	22.8	17.3
LBL-27.9-56	77.7	0.0215	29.2	23.3
LBL-13.4-57	37.6	0.0360	17.5	14.3
LBL-15.0-61	42.5	0.0331	19.0	15.4
LBL-12.4-61	35.1	0.0371	17.0	13.6
LBL-14.7-62	41.9	0.0357	17.6	15.2
LBL-23.9-64	68.3	0.0233	27.0	21.0
LBL-28.7-69	83.6	0.0211	29.8	23.7
LBL-20.0-73	59.5	0.0282	22.3	18.7
LBL-25.8-75	77.0	0.0224	28.0	22.0
mLBL-33.6-37	60.4	0.0286	21.9	20.6
mLBL-25.3-48	50.7	0.0326	19.3	17.9
mLBL-23.4-51	48.5	0.0346	18.2	17.2
mLBL-21.4-55	46.2	0.0362	17.4	16.5
mLBL-19.8-59	44.2	0.0375	16.8	15.9
mLBL-17.9-64	42.0	0.0397	15.8	15.2
mLBL-17.8-64	41.9	0.0402	15.6	15.1

[a]Segregation strength calculated using χ_{LB} = 0.1924 at T_{ref} = 155 °C. [b]Primary scattering peak position determined from synchrotron SAXS at 120 °C. [c]Experimentally determined $d = 2\pi/q^*$. [d]Theoretically calculated *d*-spacing for the equivalent mLB diblock copolymer with $N_{di} = N_{total}/2$ from strong segregation theory.[61]

molecular weights and compositions. We also used the formalism developed by Matsen and Bates for monodisperse copolymers[61] to calculate the theoretically expected *d*-spacings for the LBL and mLBL series as

$$d_{thy} = \frac{4}{\sqrt{6}}\left(\frac{3}{\pi^2}\right)^{1/3} a N_{di}{}^{2/3}\chi^{1/6}$$

where a is the volume fraction weighted root-mean-square average of the statistical segment lengths, $a = (a_B{}^2 * f_B + a_L{}^2 * (1 - f_B))^{1/2}$, and $N_{di} = N_{total}/2$ is the equivalent diblock degree of polymerization. (Note: our use of the volume fraction-weighted average statistical segment length accounts for the systematic variation in f_B among the samples presented here.) While the mLBL *d*-spacings are ∼5% larger than the theoretically calculated values as expected, the broad dispersity LBL *d*-spacings are ∼3−32% larger than theoretically expected for their narrow dispersity analogues with the same M_n. From the plot of log(*d*) versus log(*N*) shown in Figure 4, we deduce that $\beta = 0.72 \pm 0.06$ for the broad dispersity LBL triblock copolymers. Although the narrow dispersity mLBL series seemingly exhibits $\beta \geq 0.66$, we note that these data derive from one series of mLBL triblock copolymers stemming from a single telechelic PB-OH_2, which results in a systematic variation f_B with *N* that accounts for this effect.

While copolymer segment dispersity is known to cause lamellar *d*-spacing dilation in A/B diblock and multiblock copolymers as compared to their narrow dispersity analogues, the reported amount of dilation varies quite widely. In their studies of weakly segregated olefin multiblock copolymers (OBCs) derived from chain shuttling polymerization catalysis in which $Đ \sim 2.0$ for each copolymer segment, Register and co-workers estimated a 5-fold increase in the *d*-spacing that manifests in the photonic properties of these semicrystalline polyolefins.[35] The OBC *d*-spacings also appear to be relatively insensitive to the overall copolymer molecular weight,

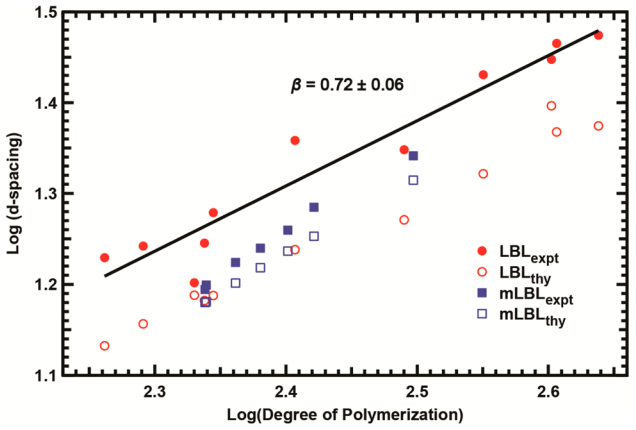

Figure 4. Lamellar mesophase domain scaling analysis for broad dispersity LBL (red circles) and narrow dispersity mLBL (blue squares) triblock copolymers. Experimental lamellar domain spacings (filled symbols) were determined from the primary SAXS peak position at T = 120 °C. Theoretical domain spacings (open symbols) were determined using previously developed expressions for monodisperse copolymers.[61]

indicating that $\beta \sim 0$ for these systems. In weakly and moderately segregated AB diblock copolymers comprising one narrow dispersity and one broad dispersity block, microdomain dilations of ∼20−50% have been reported.[30,34,62] Further experiments by Lynd and Hillmyer indicate that strongly segregated AB dibock copolymers with one broad dispersity segment display ∼10−30% dilation.[30] Mahanthappa and co-workers found that B segment dispersities $Đ \sim 1.70$−2.00 in weakly segregated ABA triblock copolymers with narrow dispersity A blocks induced domain dilations of ∼2−2.5 times as compared to narrow dispersity copolymers.[37,39] However, the limited number of lamellar samples reported in these model studies precludes the quantitative determination of β for these systems. The lower degrees of domain dilation observed in the more strongly segregated LBL copolymers suggest that the extent of domain dilation correlates with the segregation strength. Self-consistent mean-field theory calculations by Matsen[40] and dissipative particle dynamics simulations by Qian and co-workers[63−65] anticipate domain dilations of only ∼10−20% in all cases. Matsen has suggested that the discrepancy between theory and experiments arises from differences in the exact shape of the experimental and theoretical molar mass distributions of the copolymers. Nonetheless, these theories do predict decreased dilation as $\chi_{AB}N$ increases.

DISCUSSION

The lamellar mesophase composition window shift to higher than expected volume fractions f_B of the broad dispersity B block in LBL triblock copolymers is consistent with previous reports on related SBS[39] and OBO[37] copolymers. The effects of B segment dispersity on ABA triblock copolymer phase behavior have been previously explained in terms of the overall copolymer molecular weight dispersity and the associated copolymer composition dispersity. The copolymer composition dispersity implies that there is a population of ABA chains with short B blocks and "average" length A blocks. If the energetic penalty for dissolving these short B blocks in the A domains is smaller than the entropic penalty associated with localizing and stretching these chains at the domain interface, then these

dx.doi.org/10.1021/ma5006233 | Macromolecules 2014, 47, 4346−4356

chains will desorb from the microdomain interface and act like "A−A homopolymers" that swell the narrow dispersity A domains.[41] By virtue of this chain desorption, the molecular weight distribution of the remaining B segments in the ABA copolymers templating the microphase-separated morphology narrows and shifts to higher values of $M_{n,B}$. Of these remaining copolymer chains, intermediate length chains occupy interfacial area that shields the highest molecular weight chains from unfavorable A/B segmental contacts. This "co-surfactancy"[66−68] of the intermediate length chains enables significant relief of chain stretching in the high molecular weight population. Relief of chain stretching in the broad dispersity B segment coupled with chain desorption and A domain swelling results in the broad dispersity B block filling *less* volume than expected based on the chemical composition of the copolymer. Furthermore, the observed *d*-spacing depends upon the average molecular weight of the B segments of copolymers that are localized at the domain interfaces within the microphase-separated morphology.

Based on the above reasoning, increasing χ_{AB} should decrease the extent of chain desorption and thus decrease the swelling of the A domains with "A−A homopolymers" (Figure 5).

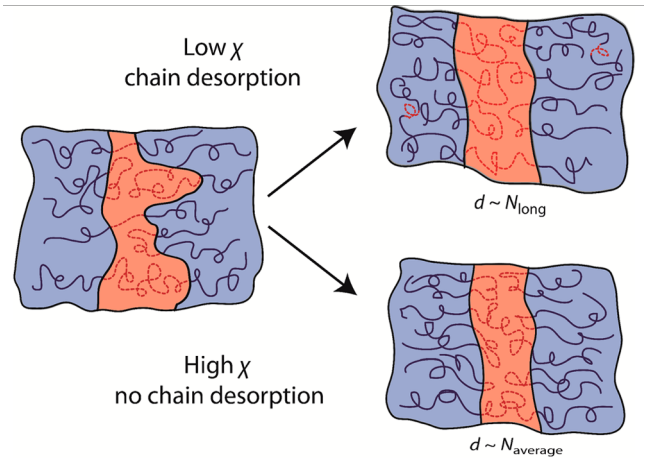

Figure 5. Chain conformations in SBS (low χ) and LBL (high χ) systems with broad dispersity center segments.

Calculations analogous to those previously reported for chain desorption in SBS and OBO copolymers suggest that only a small percentage (≤5% at 155 °C) of LBL chains desorb from the microphase-separated domain interfaces. Decreased chain desorption lowers the average molar mass of the B segments of the ABA copolymers that template the observed *d*-spacing. In other words, χ_{AB} directly affects the molar mass cutoff above which ABA triblock copolymer chains participate in the morphology and influence the observed *d*-spacing; a larger χ_{AB} decreases the molar mass cutoff and allows more of the low molecular weight chains to dictate the *d*-spacing. These two effects thus conspire to reduce the expected amount of domain dilation in a high χ_{AB} block copolymer system as compared to one with a small χ_{AB}. (One would also expect that a strongly temperature-dependent $\chi_{AB}(T)$ should lead to substantial changes in the critical molecular weight cutoff for chain desorption as a function of temperature, which should manifest in a temperature-dependent *d*-spacing. However, we do not observe any such effect.) This conceptual framework is consistent with the reduced domain dilation observed in high χ LBL copolymers as compared to lower χ OBO and SBS copolymers. Furthermore, one would anticipate that the lamellar *d*-spacings for high χ_{AB} broad and narrow dispersity copolymer melts might exhibit similar scalings with respect to the average *N* (derived from the number-average molecular weight $M_{n,total}$ for the copolymer). This notion is also consistent with our observation that $d \propto N^{0.72\pm0.06}$ for the broad dispersity LBL copolymers, as compared to the expected $d \propto N^{2/3}$ from strong segregation theories for monodisperse copolymers. Therefore, we conclude that chain desorption is a major factor that dictates the extent of dilation of the microphase separated domains of broad dispersity ABA triblock copolymers.

In spite of their very different amounts of chain desorption and different conformational asymmetries, the coincident locations of the lamellar mesophase composition windows for broad dispersity LBL and SBS copolymers in the range $0.52 \leq f_B \leq 0.75$ suggest that cosurfactancy drives the shift in the composition-dependent morphology window. Since nearly all of the chains in the broad dispersity LBL melts sit at the domain interfaces, even the smallest chains in the broad molar mass distribution must exert a substantial cosurfactant effect that overrides the formation of the morphology expected based solely on volume filling considerations. Recent calculations by Matsen on ABA copolymers[40] with broad dispersity B segments quantitatively concur with these experimental observations, in spite of the previously noted discrepancies in the observed and predicted domain spacings.

CONCLUSION

A series of 11 lamellar LBL triblock copolymers with broad dispersity center segments were synthesized by tandem ROMP-CT of cyclododecatriene and ROTEP of lactide. Complete molecular characterization of each block by SEC and ^{1}H NMR demonstrates the controlled, yet polydisperse nature of the center B block that is flanked by narrow dispersity L end blocks. Based on temperature-dependent SAXS analyses, the Flory−Huggins interaction parameter was determined to be $\chi_{LB} = 0.1924$ at 155 °C. The observed lamellar *d*-spacings for polydisperse LBL copolymers are only modestly dilated as compared to their narrow dispersity analogues and they scale as $d \propto N^{0.72}$, consistent with strong segregation theories for monodisperse copolymers. This behavior may be rationalized in terms of the low degree of χ-dependent chain desorption and mixing in these high χ block copolymers. However, broad center segment dispersity in LBL triblocks leads to cosurfactant effects that drive a substantial shift in the lamellar microphase composition window to the range $f_B = 0.52−0.75$. This work reveals the crucial role of χ in dictating the morphological behavior of ABA triblock copolymers with broad B block dispersities, which will be crucial for the design of polydisperse yet functional polymeric materials.

ASSOCIATED CONTENT

Supporting Information

SEC analyses of LBL-27.9-56, azimuthally integrated synchrotron SAXS patterns for LBL-12.5-44 and LBL-18.2-79, and detailed procedure for determining χ_{LB} from synchrotron SAXS data. This material is available free of charge via the Internet at http://pubs.acs.org.

AUTHOR INFORMATION

Corresponding Author

*E-mail mahesh@chem.wisc.edu; Tel +1 (608) 262-0421 (M.K.M.).

Notes

The authors declare no competing financial interest.

■ ACKNOWLEDGMENTS

We gratefully acknowledge financial support from the National Science Foundation (DMR-1307606) and the University of Wisconsin—Madison. This research relied upon NSF MRSEC and NSF NSEC core characterization facilities UW—Madison (DMR-0832760 and DMR-1121288). Synchrotron SAXS analyses (GUP No. 75709 and 25134) were conducted at the DuPont−Northwestern−Dow Collaborative Access Team (DND-CAT) located at Sector 5 of the Advanced Photon Source (APS), supported by E.I. DuPont de Nemours & Co., the Dow Chemical Company, and Northwestern University. Use of the APS, an Office of Science User Facility operated for the U.S. Department of Energy (DOE) Office of Science by Argonne National Laboratory, was supported by the U.S. DOE under Contract DE-AC02-06CH11357.

■ REFERENCES

(1) Bates, F. S.; Hillmyer, M. A.; Lodge, T. P.; Bates, C. M.; Delaney, K. T.; Fredrickson, G. H. *Science* **2012**, *336*, 434−440.
(2) Ruzette, A.-V.; Leibler, L. *Nat. Mater.* **2005**, *4*, 19−31.
(3) Abetz, V.; Simon, P. F. W. *Adv. Polym. Sci.* **2005**, *190*, 125−212.
(4) Leibler, L. *Macromolecules* **1980**, *13*, 1602−1617.
(5) Cochran, E. W.; Garcia-Cervera, C. J.; Fredrickson, G. H. *Macromolecules* **2006**, *39*, 2449−2451.
(6) Matsen, M. W. *Macromolecules* **2012**, *45*, 2161−2165.
(7) Matsen, M. W.; Bates, F. S. *Macromolecules* **1996**, *29*, 1091−1098.
(8) Lodge, T. P.; Hillmyer, M. A.; Zhou, Z.; Talmon, Y. *Macromolecules* **2004**, *37*, 6680−6682.
(9) Davidock, D. A.; Hillmyer, M. A.; Lodge, T. P. *Macromolecules* **2003**, *36*, 4682−4685.
(10) Semenov, A. N. *Macromolecules* **1993**, *26*, 6617−6621.
(11) Matsen, M. W.; Schick, M. *Macromolecules* **1994**, *27*, 187−192.
(12) Khandpur, A. K.; Foerster, S.; Bates, F. S.; Hamley, I. W.; Ryan, A. J.; Bras, W.; Almdal, K.; Mortensen, K. *Macromolecules* **1995**, *28*, 8796−8806.
(13) Mai, S.-M.; Mingvanish, W.; Turner, S. C.; Chaibundit, C.; Fairclough, J. P. A.; Heatley, F.; Matsen, M. W.; Ryan, A. J.; Booth, C. *Macromolecules* **2000**, *33*, 5124−5130.
(14) Papadakis, C. M.; Almdal, K.; Mortensen, K.; Posselt, D. *Europhys. Lett.* **1996**, *36*, 289.
(15) Matyjaszewski, K.; Xia, J. *Chem. Rev.* **2001**, *101*, 2921−2990.
(16) Ouchi, M.; Terashima, T.; Sawamoto, M. *Chem. Rev.* **2009**, *109*, 4963−5050.
(17) Moad, G.; Rizzardo, E.; Thang, S. H. *Polymer* **2008**, *49*, 1079−1131.
(18) David, G.; Boyer, C.; Tonnar, J.; Ameduri, B.; Lacroix-Desmazes, P.; Boutevin, B. *Chem. Rev.* **2006**, *106*, 3936−3962.
(19) Hillmyer, M. *Curr. Opin. Solid State Mater. Sci.* **1999**, *4*, 559−564.
(20) Bielawski, C. W.; Morita, T.; Grubbs, R. H. *Macromolecules* **2000**, *33*, 678−680.
(21) Leolukman, M.; Paoprasert, P.; Wang, Y.; Makhija, V.; McGee, D. J.; Gopalan, P. *Macromolecules* **2008**, *41*, 4651−4660.
(22) Zalusky, A. S.; Olayo-Valles, R.; Wolf, J. H.; Hillmyer, M. A. *J. Am. Chem. Soc.* **2002**, *124*, 12761−12773.
(23) Anderson, K. S.; Schreck, K. M.; Hillmyer, M. A. *Polym. Rev.* **2008**, *48*, 85−108.
(24) Lipscomb, C. E.; Mahanthappa, M. K. *Macromolecules* **2009**, *42*, 4571−4579.
(25) Wanamaker, C. L.; Tolman, W. B.; Hillmyer, M. A. *Biomacromolecules* **2009**, *10*, 443−448.
(26) Arriola, D. J.; Carnahan, E. M.; Hustad, P. D.; Kuhlman, R. L.; Wenzel, T. T. *Science* **2006**, *312*, 714−719.
(27) Hustad, P. D.; Marchand, G. R.; Garcia-Meitin, E. I.; Roberts, P. L.; Weinhold, J. D. *Macromolecules* **2009**, *42*, 3788−3794.
(28) Li, S.; Register, R. A.; Landes, B. G.; Hustad, P. D.; Weinhold, J. D. *Macromolecules* **2010**, *43*, 4761−4770.
(29) Lynd, N. A.; Hamilton, B. D.; Hillmyer, M. A. *J. Polym. Sci., Part B: Polym. Phys.* **2007**, *45*, 3386−3393.
(30) Lynd, N. A.; Hillmyer, M. A. *Macromolecules* **2005**, *38*, 8803−8810.
(31) Lynd, N. A.; Hillmyer, M. A. *Macromolecules* **2007**, *40*, 8050−8055.
(32) Lynd, N. A.; Meuler, A. J.; Hillmyer, M. A. *Prog. Polym. Sci.* **2008**, *33*, 875−893.
(33) Bendejacq, D.; Ponsinet, V.; Joanicot, M.; Loo, Y. L.; Register, R. A. *Macromolecules* **2002**, *35*, 6645−6649.
(34) Ruzette, A.-V.; Tence-Girault, S.; Leibler, L.; Chauvin, F.; Bertin, D.; Guerret, O.; Gerard, P. *Macromolecules* **2006**, *39*, 5804−5814.
(35) Li, S.; Register, R. A.; Weinhold, J. D.; Landes, B. G. *Macromolecules* **2012**, *45*, 5773−5781.
(36) Banik, S. M.; Monnot, B. L.; Weber, R. L.; Mahanthappa, M. K. *Macromolecules* **2011**, *44*, 7141−7148.
(37) Schmitt, A. L.; Mahanthappa, M. K. *Soft Matter* **2012**, *8*, 2294−2303.
(38) Widin, J. M.; Schmitt, A. K.; Im, K.; Schmitt, A. L.; Mahanthappa, M. K. *Macromolecules* **2010**, *43*, 7913−7915.
(39) Widin, J. M.; Schmitt, A. K.; Schmitt, A. L.; Im, K.; Mahanthappa, M. K. *J. Am. Chem. Soc.* **2012**, *134*, 3834−3844.
(40) Matsen, M. W. *Eur. Phys. J. E: Soft Matter* **2013**, *36*, 1−7.
(41) Matsen, M. W. *Eur. Phys. J. E: Soft Matter* **2006**, *21*, 199−207.
(42) Pitet, L. M.; Hillmyer, M. A. *Macromolecules* **2009**, *42*, 3674−3680.
(43) Meuler, A. J.; Mahanthappa, M. K.; Hillmyer, M. A.; Bates, F. S. *Macromolecules* **2007**, *40*, 760−762.
(44) Brandrup, J.; Immergut, E. H.; Grulke, E. A. *Polymer Handbook*, 4th ed.; Wiley-Interscience: New York, 1999.
(45) Henton, D. E.; Gruber, P.; Lunt, J.; Randall, J. Polylactic acid technology. In *Natural Fibers, Biopolymers, and Biocomposites*; Mohanty, A. K., Misra, M., Drzal, L. T., Eds.; Taylor & Francis: Boca Raton, FL, 2005; pp 527−577.
(46) Schmitt, A. K.; Mahanthappa, M. K. Computer Code for Materials Scientists: Igor Pro Procedures for Analyzing Dynamic Light Scattering, Rheology, and Synchrotron X-ray Scattering Data. figShare http://dx.doi.org/10.6084/m9.figshare.644515.
(47) Lohmeijer, B. G. G.; Pratt, R. C.; Leibfarth, F.; Logan, J. W.; Long, D. A.; Dove, A. P.; Nederberg, F.; Choi, J.; Wade, C.; Waymouth, R. M.; Hedrick, J. L. *Macromolecules* **2006**, *39*, 8574−8583.
(48) Mahanthappa, M. K.; Bates, F. S.; Hillmyer, M. A. *Macromolecules* **2005**, *38*, 7890−7894.
(49) Barton, A. F. M. *Handbook of Solubility Parameters and Other Cohesion Parameters*, 2nd ed.; CRC Press: Boca Raton, FL, 1991.
(50) Karst, D.; Yang, Y. *J. Appl. Polym. Sci.* **2005**, *96*, 416−422.
(51) Rosedale, J. H.; Bates, F. S.; Almdal, K.; Mortensen, K.; Wignall, G. D. *Macromolecules* **1995**, *28*, 1429−1443.
(52) Maurer, W. W.; Bates, F. S.; Lodge, T. P.; Almdal, K.; Mortensen, K.; Fredrickson, G. H. *J. Chem. Phys.* **1998**, *108*, 2989−3000.
(53) Cochran, E. W.; Bates, F. S. *Macromolecules* **2002**, *35*, 7368−7374.
(54) Lee, S.; Gillard, T. M.; Bates, F. S. *AIChE J.* **2013**, *59*, 3502−3513.
(55) Fetters, L. J.; Lohse, D. J.; Richter, D.; Witten, T. A.; Zirkel, A. *Macromolecules* **1994**, *27*, 4639−4647.
(56) Witzke, D. R.; Narayan, R.; Kolstad, J. J. *Macromolecules* **1997**, *30*, 7075−7085.
(57) Lee, I.; Panthani, T. R.; Bates, F. S. *Macromolecules* **2013**, *46*, 7387−7398.

(58) Bielawski, C. W.; Hillmyer, M. A. Telechelic Polymers from Olefin Metathesis Methodologies. In *Handbook of Metathesis*; Grubbs, R. H., Ed.; Wiley-VCH: Weinheim, 2003; Vol. *3*, pp 255−281.
(59) Bielawski, C. W.; Benitez, D.; Grubbs, R. H. *J. Am. Chem. Soc.* **2003**, *125*, 8424−8425.
(60) Schmitt, A. L.; Repollet-Pedrosa, M. H.; Mahanthappa, M. K. *ACS Macro Lett.* **2012**, *1*, 300−304.
(61) Matsen, M. W.; Bates, F. S. *J. Chem. Phys.* **1997**, *106*, 2436−2448.
(62) Widin, J. M.; Kim, M.; Schmitt, A. K.; Han, E.; Gopalan, P.; Mahanthappa, M. K. *Macromolecules* **2013**, *46*, 4472−4480.
(63) Li, Y.; Qian, H.-J.; Lu, Z.-Y. *Polymer* **2013**, *54*, 3716−3722.
(64) Li, Y.; Qian, H. J.; Lu, Z. Y. *Europhys. Lett.* **2013**, *103*, 68001.
(65) Li, Y.; Qian, H.-J.; Lu, Z.-Y.; Shi, A.-C. *J. Chem. Phys.* **2013**, *139*, 096101.
(66) Court, F.; Hashimoto, T. *Macromolecules* **2002**, *35*, 2566−2575.
(67) Court, F.; Yamaguchi, D.; Hashimoto, T. *Macromolecules* **2006**, *39*, 2596−2605.
(68) Court, F.; Yamaguchi, D.; Hashimoto, T. *Macromolecules* **2008**, *41*, 4828−4837.